Cement & Concrete Composites 30 (2008) 798–805

Contents lists available at ScienceDirect

Cement & Concrete Composites

journal homepage: www.elsevier.com/locate/cemconcomp

Ceramic wastes as alternative raw materials for Portland cement clinker production

F. Puertas [a,*], I. García-Díaz [a], A. Barba [b], M.F. Gazulla [b], M. Palacios [a], M.P. Gómez [b], S. Martínez-Ramírez [a]

[a] Eduardo Torroja Institute for Construction Sciences (CSIC), Madrid, Spain
[b] Institute of Ceramic Technology, Jaume I University, Castellon, Spain

ARTICLE INFO

Article history:
Received 6 February 2007
Received in revised form 13 May 2008
Accepted 8 June 2008
Available online 19 June 2008

Keywords:
Cement manufacture
Alternative raw mixes
Ceramic waste
Reactivity
Traces elements

ABSTRACT

The cement industry has for some time been seeking procedures that would effectively reduce the high energy and environmental costs of cement manufacture. One such procedure is the use of alternative materials as partial replacements for fuel, raw materials or even clinker. The present study explores the reactivity and burnability of cement raw mixes containing fired red or white ceramic wall tile wastes and combinations of the two as alternative raw materials.

The results showed that the new raw mixes containing this kind of waste to be technically viable, and to have higher reactivity and burnability than a conventional mix, providing that the particle size of the waste used is lower than 90 μm. The mineralogical composition and distribution in the experimental clinker prepared were comparable to the properties of the clinker manufactured with conventional raw materials. Due to the presence of oxides such as ZnO, ZrO_2 and B_2O_3 in tile glazing, the content of these oxides was higher in clinker made with such waste. The mix of red and white ceramic wall tile waste was found to perform equally or better than each type of waste separately, a promising indication that separation of the two would be unnecessary for the purpose described above.

1. Introduction

Portland cement clinker production consumes large amounts of energy (850 kcal per kg of clinker) and has a considerable environmental impact. This involves massive quarrying for raw materials (limestone, clay, etc.), as it takes 1.7 tonnes to produce 1 tonne of clinker, as well as the emission of greenhouse and other gases (NO_x, SO_2, CO_2) into the atmosphere. Around 850 kg of CO_2 are emitted per tonne of clinker produced.

The cement industry is looking for solutions to these problems, to attain sustainability and comply with the Kyoto Protocol commitments [1,2]. For that reason, experimental ways are being explored to develop cements whose manufacture is less energy-intensive, less damaging to the surrounding environment and with lower tendency to emit polluting gas. One way to reach this objective is the use of industrial waste and by-products as alternative materials for cement manufacture. Such alternative materials may partially replace fuel [3,4], conventional raw materials [5–10] or clinker in the final composition of the cement [11–13].

A recent study [14] showed that the chemical and mineralogical composition of certain types of ceramic wastes are appropriate for inclusion in raw cement mixes. Such wastes are generated in tile plants. As a result of an increasing demand for tile on the Spanish market, production has grown to over 600 million m^2 per year, with a parallel increase of solid waste, which currently is estimated to over 50,000 tonnes annually. Since the re-use of such waste in tile manufacture itself is not technically viable, they are deposited in regulated dumping grounds, creating an environmental problem.

Reports have been published on the suitability of certain types of ceramic waste as supplementary cementing materials [15,16], together with clinker; there are no studies, however, on the use of such waste in the manufacture of Portland cement clinker itself. Consequently, the aim of the present research was to study the reactivity and burnability of Portland cement raw mixes containing ceramic wastes as a partial substitute for conventional raw materials.

2. Experimental

2.1. Materials

Three types of red ceramic tile wastes were chosen:

R–R = Fired red ceramic wall tile.
R–B = Fired white ceramic wall tile.
R–M = Combination of red and white ceramic wall tile (i.e. unseparated ceramic waste).

Ceramic wall tile wastes with an initial size higher than 5 mm were crushed using a jaw crusher. Subsequently the ceramic

* Corresponding author. Tel.: +34 913020440; fax: +34 913020700.
E-mail address: puertasf@ietcc.csic.es (F. Puertas).

0958-9465/$ - see front matter © 2008 Elsevier Ltd. All rights reserved.
doi:10.1016/j.cemconcomp.2008.06.003

Table 1
Waste particle size distribution: $X > 90$ μm fraction

Waste	d_{10} (μm)	d_{50} (μm)	d_{90} (μm)
R–R	123.98	291.79	560.55
R–B	121.12	306.46	588.73
R–M	142.90	332.41	613.19

wastes were grinded by hammer mill. Ceramic wastes were sieved in order to obtain three particle size fractions, as follows:

1. All particles smaller than 45 μm ($X < 45$ μm).
2. Particle size ranging from 45 to 90 μm ($45 < X < 90$ μm).
3. All particles larger than 90 μm ($X > 90$ μm).

Table 1 gives the particle size distribution for this last fraction.

The mean chemical composition for each type of waste and fraction is shown in Table 2. Table 3 provides the mineralogical composition of these tiles as found with X-ray diffraction (XRD) techniques.

To be able to evaluate the effect of particle size distribution of the ceramic waste on raw mix reactivity and burnability, a constant particle size, based on Miller's [17] findings, was used for all other raw materials throughout. Limestone particle size was consistently smaller than 125 μm, while sand and clay particles were smaller than 45 μm. The chemical analysis of these materials is shown in Table 4. Ferric oxide (96% pure, Panreac chemical reagent) was used to correct the iron content.

2.2. Raw mix preparation

The following parameters were constant in all the mixes and they were adjusted according to Eqs. (1)–(3):

$$\mathrm{LSF} = (\mathrm{CaO}/2.8\mathrm{SiO_2} + 1.18\mathrm{Al_2O_3} + 0.65\mathrm{Fe_2O_3}) \times 100 = 98\%, \quad (1)$$

$$\mathrm{Ms} = \mathrm{SiO_2}/\mathrm{Fe_2O_3} + \mathrm{Al_2O_3} = 2.30, \quad (2)$$

$$\mathrm{Mf} = \mathrm{Al_2O_3}/\mathrm{Fe_2O_3} = 1.50. \quad (3)$$

where LSF is the lime saturation factor, Ms is the silica modulus and Mf is the meeting modulus.

One raw mix was prepared for each fraction of the three types of ceramic waste, along with one reference raw mix containing no waste. Table 5 gives the percentage composition of these raw mixes.

Given the minor differences between the global chemical composition and each particle size fraction of ceramic wall tile (see Table 2), the raw mixes were prepared considering the global chemical composition.

The raw mixes were prepared as follows: after in a turbula for 60 min, the components were stirred in a suspension with ethanol in an agate mortar for 30 min, not to alter the pre-established particle size distribution. The excess of ethanol was removed by heating the mix under an infrared lamp. Tablets weighing around 4–5 g each and 3 cm in diameter were prepared from each raw mix and then clinkerized at the following temperatures: 1270 °C, 1350 °C, 1400 °C, 1450 °C, and 1500 °C. The samples were heated at each temperature for 30 min and then cooled at ambient temperature.

Table 2
Global chemical composition of the ceramic waste and respective fractions

(wt. %)	Ppc	SiO_2	Al_2O_3	Fe_2O_3	CaO	MgO	Na_2O	K_2O	TiO_2	MnO	P_2O_5	ZnO	ZrO_2	SO_3
$R–R_{(GLOBAL)}$	0.36	63.8	17.4	3.55	6.55	1.90	1.27	3.05	0.61	0.04	0.23	0.35	0.5	0.06
$R–R_{(X < 45\ \mu m)}$	0.32	65.2	17.3	3.36	6.35	1.73	1.35	2.83	0.59	0.03	0.20	0.12	0.31	0.04
$R–R_{(45 < X < 90\ \mu m)}$	0.48	65.0	17.2	3.37	6.25	1.76	1.29	2.99	0.56	0.04	0.22	0.20	0.35	0.04
$R–R_{(X > 90\ \mu m)}$	0.32	62.9	17.7	3.64	6.70	2.01	1.22	3.19	0.65	0.05	0.25	0.54	0.67	0.08
$R–B_{(GLOBAL)}$	0.48	64.8	18.0	1.82	9.92	0.42	0.62	2.09	0.70	0.01	0.21	0.42	0.31	0.13
$R–B_{(X < 45\ \mu m)}$	0.34	64.7	18.5	1.92	10.25	0.38	0.44	2.05	0.71	0.01	0.21	0.14	0.14	0.16
$R–B_{(45 < X < 90\ \mu m)}$	0.27	65.9	17.7	1.89	9.68	0.38	0.46	1.94	0.70	0.01	0.20	0.25	0.19	0.14
$R–B_{(X > 90\ \mu m)}$	0.36	64.1	18.2	1.67	9.83	0.47	0.83	2.14	0.68	0.01	0.21	0.70	0.49	0.11
$R–M_{(GLOBAL)}$	0.29	62.2	16.8	4.7	6.75	2.71	0.81	3.95	0.67	0.04	0.17	0.36	0.32	0.05
$R–M_{(X < 45\ \mu m)}$	0.25	61.5	17.1	4.87	7.11	2.87	0.77	3.99	0.66	0.05	0.21	0.26	0.24	0.05
$R–M_{(45 < X < 90\ \mu m)}$	0.15	63.0	16.3	4.40	6.67	2.55	0.81	3.78	0.66	0.04	0.18	0.31	0.25	0.04
$R–M_{(X > 90\ \mu m)}$	0.37	61.4	16.8	4.63	6.88	2.63	0.85	4.27	0.67	0.04	0.19	0.52	0.38	0.02

(mg Kg^{-1})	PbO	BaO	B_2O_3	Cr_2O_3	V_2O_5	Co_3O_4	NiO	CuO	As_2O_3	Sb_2O_3	CdO
$R–R_{(GLOBAL)}$	290	1000	1370	115	129	<20	<20	<20	<20	<20	<20
$R–R_{(X < 45\ \mu m)}$	230	1300	1100	95	100	<20	<20	<20	<20	<20	<20
$R–R_{(45 < X < 90\ \mu m)}$	275	1300	1300	110	120	<20	<20	<20	<20	<20	<20
$R–R_{(X > 90\ \mu m)}$	320	700	1500	125	140	<20	<20	<20	<20	<20	<20
$R–B_{(GLOBAL)}$	150	600	1830	120	118	<20	<20	<20	<20	<20	<20
$R–B_{(X < 45\ \mu m)}$	100	<0.01(%)	1590	80	75	<20	<20	<20	<20	<20	<20
$R–B_{(45 < X < 90\ \mu m)}$	130	400	1750	110	105	<20	<20	<20	<20	<20	<20
$R–B_{(X > 90\ \mu m)}$	190	800	1900	150	145	<20	<20	<20	<20	<20	<20
$R–M_{(GLOBAL)}$	125	485	1835	59	150	<20	<20	<20	<20	<20	<20
$R–M_{(X < 45\ \mu m)}$	91	500	1350	40	110	<20	<20	<20	<20	<20	<20
$R–M_{(45 < X < 90\ \mu m)}$	103	500	1500	50	125	<20	<20	<20	<20	<20	<20
$R–M_{(X > 90\ \mu m)}$	125	700	1840	60	150	<20	<20	<20	<20	<20	<20

Table 3
Mineralogical composition of ceramic waste (% by weight)

Waste	Quartz	Anorthite	K feldespar	Albite	Hematites	Diopside	Gehlenite	Zircon	Wollastonite	Amorphous phase
R–R	33	24	8	4	3	3	1	1	<1	24
R–B	37	32	8	5	1	<1	1	<1	6	9
R–M	26	14	8	3	3	5	1	1	4	34

Table 4
Chemical composition of the other prime materials used in the raw mix

(wt. %)	ppc (1025 °C)	SiO_2	Al_2O_3	Fe_2O_3	CaO	MgO	Na_2O	K_2O	TiO_2	MnO	P_2O_5	ZnO	ZrO_2	SO_3
Limestone	40.5	5.6	1.3	0.58	51.1	0.58	<0.01	0.23	0.07	0.01	0.10	<20 mg/kg	<20 mg/kg	–
Sand	2.09	89.4	3.90	0.61	2.06	0.03	0.07	1.79	0.04	<0.01	0.03	<20 mg/kg	<20 mg/kg	–
Clay	9.20	52.0	15.1	6.02	4.01	4.95	0.58	4.55	0.73	0.10	0.15	<20 mg/kg	<20 mg/kg	2.6

(mg Kg^{-1})	PbO	BaO	B_2O_3	Cr_2O_3	V_2O_5	Co_3O_4	NiO	CuO	As_2O_3	Sb_2O_3	CdO
Limestone	<20	<20	<20	<20	57	<20	<20	<20	<20	<20	<20
Sand	<20	<20	<20	468	<20	<20	<20	<20	<20	<20	<20
Clay	<20	725	480	75	195	<20	<20	<20	<20	<20	<20

Table 5
Raw mix composition (% by weight)

Raw mat.	Reference	R–R	R–B	R–M
Limestone	82.35	83.72	83.90	83.42
Clay	16.15	3.47	–	4.74
Sand	0.6	–	–	–
Fe_2O_3	0.91	1.31	1.71	1.13
Waste	–	11.47	14.39	10.70

2.3. Tests conducted

Differential thermal (DTA) and thermogravimetric (TG) analyses were run on the raw mixes with an STA 409 thermal analyzer. Samples weighing 250 mg were heated at a rate of 4 °C/min to a maximum temperature of 1500 °C. The cooling rate was 10 °C/min.

The following tests were conducted on the clinker obtained:

(a) Chemical analysis, determining the component elements, Si, Al, Fe, Na, K, Ca, Mg, Ti, Mn, P, S and Zr, with a PANALYTICAL PW 2400 dispersive-wavelength X-ray fluorescence spectrometer. Pb, Zn, Ba, Cr, B, V, Co, Ni, Cu, As, Sb and Cd were determined with a LEEMAN LABS INC. Direct Reading Echelle inductively coupled plasma-optical emission spectrometer (ICP-OES).
(b) Determination of the free lime as described in Spanish standard UNE 80-24386.
(c) XRD mineralogical analysis using a PHILIPS PW 1710 diffractometer. Samples were ground to a particle size lower than 45 μm. At 2θ diffraction angles ranging from 5° to 60° using a step of 0.020.
(d) Morphological analysis a Nikon Eclipse ME600 reflected light microscope, for which the clinker was previously encapsulated in epoxy resin, cut and polished.

3. Results and discussion

The reactivity and burnability of the raw mixes containing ceramic wastes were evaluated, in order to know the viability of the use of these alternative raw materials as a partial substitute for conventional raw materials. Also the content of minor components on clinkers due to the presence of these wastes in the raw mixes was evaluated. In the following, the results obtained and their interpretations are presented.

3.1. Raw mix reactivity

Raw mix reactivity is defined by the overall reaction rate at a temperature that enables the reaction to reach completion within a reasonable time. This parameter depends on the chemical composition of the mix, the nature of the mineralogical species and the particle size.

The main difference among the raw mixes containing ceramic waste was the particle size of this component. Mix behaviour was studied with DTA. The resulting heating curves are shown in Fig. 1.

The graph on the left shows endothermal signals in the 780–900 °C range, attributed to thermal decomposition (decarbonation) of the limestone present in the mix. The DTA curves for the raw mixes containing the R–B ceramic waste exhibit a wide endothermal signal between 875 and 885 °C, comparable to the signal in the reference mix; however in the R–R and to a smaller extent in the R–M mixes, limestone decomposition temperature appears to be affected by the nature and particle size of the waste. The DTA curves for the lower than 45 μm fraction of these types of waste (R–R, R–M) present an endothermal signal at 870 °C, along with other less intense signals at higher temperatures (around 880 °C). This appears to indicate that the finer fractions of these wastes hasten limestone decomposition slightly, due perhaps to their higher Fe_2O_3 content and different mineralogical composition, the amorphous phase content (see Table 3). The raw mix containing R–R ($45 < X < 90$ μm) also exhibits other, less intense endothermal signals at lower temperatures (846–852 °C) attributed to decarbonation due to internal heterogeneity.

The exothermal signals between 1220 and 1270 °C (right-hand graph) could be attributed to solid state reactions and the progressive formation of belite, gehlenite, $C_{12}A_7$, C_3A and C_4AF [18]. The appearance of these signals at lower temperatures on the graphs, particularly for the lower than 45 μm fractions of mixes containing R–R or R–M wastes, is a sign of a slight higher reactivity.

Endothermal signals associated with melt taking place within the clinker and the initial formation of alite crystals appeared at temperatures of over 1300 °C. The endothermal signal between 1310 and 1340 °C is attributed essentially to the quaternary eutectic in the $CaO–SiO_2–Al_2O_3–Fe_2O_3$ system, in the $C_3S–C_2S–C_3A–C_4AF$ system it appears at 1338 °C [19]. The temperature and intensity of this signal was also affected by the particle size of the ceramic waste in the raw mix. This liquid phase was found to form at a higher temperature in the reference mix than in any of the waste-containing mixes when the particle size of the waste was lower than 90 μm, confirming these results newly the slight higher reactivity of the raw mix with R–R and R–M wastes. The signal was also observed to be more intense on the DTA cooling curves for the same mixes. The above observations were quantified by finding the ratios between the areas of the exothermal crystallization signals (between 1140 and 1420 °C) on the DTA cooling curves for the waste-bearing mixes (see Fig. 2) and the areas on the curves for the reference mixes. The results obtained are shown in Table 6.

The values of these ratios are an indication of the amount of liquid phase formed in the clinker obtained from ceramic wastes in raw mixes to respect to reference clinker. Analysis of the data in Table 6 show that, with one exception (the R–R mix ($X < 45$ μm)), when the ceramic waste in the raw mix had particles smaller than 90 μm, more liquid phase was formed than in the reference mix. The reason for this higher liquid phase content may lie in the

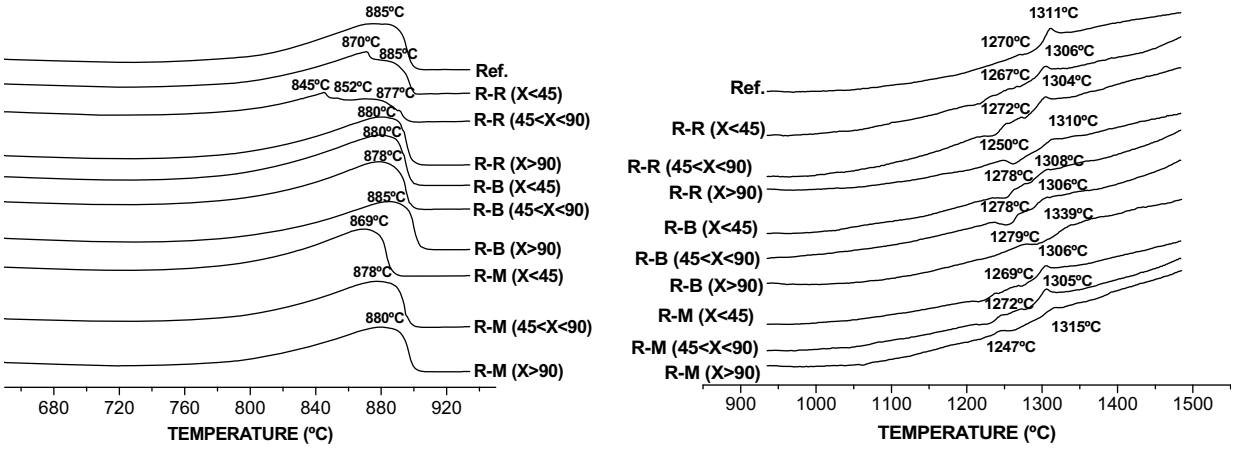

Fig. 1. DTA heating curves.

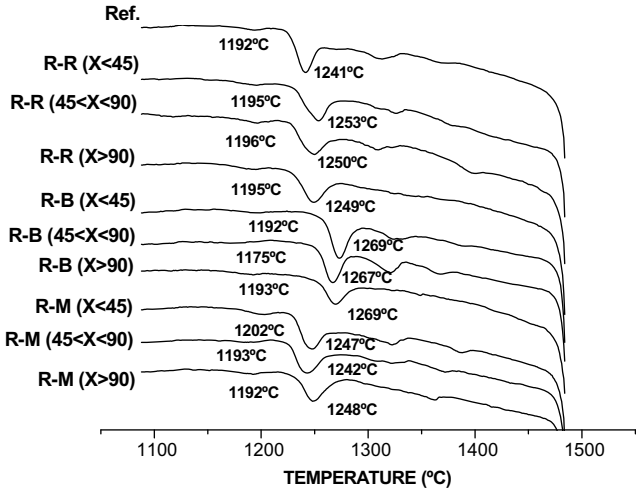

Fig. 2. DTA cooling curves.

Table 6
Ratios between the areas of exothermal signals between 1140 and 1420 °C on DTA cooling curves

	$Area_{waste}/Area_{ref}$
$R–R_{(X < 45\ \mu m)}$	0.97
$R–R_{(45 < X < 90\ \mu m)}$	1.09
$R–R_{(X > 90\ \mu m)}$	0.84
$R–B_{(X < 45\ \mu m)}$	1.12
$R–B_{(45 < X < 90\ \mu m)}$	1.06
$R–B_{(X > 90\ \mu m)}$	0.65
$R–M_{(X < 45\ \mu m)}$	1.10
$R–M_{(45 < X < 90\ \mu m)}$	1.03
$R–M_{(X > 90\ \mu m)}$	0.91

greater burnability of the fired clay in ceramic waste than of the clay used to prepare the reference mix, and the existence in the former of minority elements that favour melt, such as ZnO [18] and B_2O_3.

In other words, when the particle size of any of the three types of ceramic waste was less than 90 μm, reactivity was higher in the alternative than in the conventional raw mix, although the difference was less pronounced when R–B waste was used. As may be inferred from Table 1, the over 90 μm fraction contained very large particles, with only 10% of the sample lower than 125 μm; this may also explain the distinctly lower reactivity of mixes containing this fraction.

Table 7 shows the results of the semi-quantitative XRD analysis conducted on the different types of clinker obtained. The characters in the cells represent the intensity of the diffraction lines analyzed and, consequently, the amount of each phase present in the respective raw mix. The diffraction lines used for the various phases were: $CaO_{(Lime)}$ – 53.84 2θ (JQDS 4-777 I/Io 44 %), C_3S – 51.88 2θ (JQDS 11-593 rhombohedral I/Io 90%, JQDS 13-272 I/Io 40 %), βC_2S – 31.06 2θ (JQDS 33-0302 I/Io 20 %), γC_2S 20.55 2θ (JQDS 31-2974 I/Io 44%), C_3A – 47.59 2θ (JQDS 32-0149 I/Io 45%), C_4AF – 33.87 2θ (JQDS 30-0226 I/Io 100) and $C_{12}A_7$ – 18.32 2θ (JQDS 9-413 I/Io 94%).

This mineralogical analysis confirms the lower reactivity of the raw mixes containing ceramic waste with particles larger than 90 μm. Mayenite ($C_{12}A_7$), for instance, was found in the clinker obtained at 1270 °C and its content was greater when the larger than 90 μm fraction was used. γ-C_2S was also detected in the clinker at this temperature. Furthermore, the clinker obtained from raw mixes containing this fraction of the waste product more free lime and belite both at all clinkerization temperatures tested.

Raw mixes containing the R–B waste exhibited lower reactivity than those containing other types of waste: the clinker obtained from raw mixes with R–B waste at temperatures up to 1400 °C had a high free lime content even when the smaller than 90 μm fraction was used.

The XRD results showed that the mineralogical composition of the clinker obtained from raw mixes containing ceramic waste was more or less similar to the composition of the reference clinker at all temperatures; moreover, no significant differences were found between R–R and R–M waste.

A morphological analysis of the clinker obtained at 1450 °C confirmed the XRD results. Fig. 3 shows the micrographs of the reference clinker and the clinker obtained at 1450 °C from raw mixes containing the three types of ceramic waste, all with a particle size lower than 45 μm. In this regard, the phase distribution and size of the R–R and R–M clinkers were comparable to the findings for the reference clinker (Fig. 3B, D). The clinker containing the R–B waste, however, showed heterogeneous alite crystal size and a higher belite phase content. These results are indicative of the lower reactivity of the R–B waste raw mix already detected.

Fig. 4 shows the micrographs of the clinker obtained at 1450 °C from raw mixes containing R–R and R–M ceramic waste, with a particle size from 45 to 90 μm. It can be detected that the phase distribution is consistent in the clinkers. The distribution of alite crystals was more uneven and the belite content higher in clinkers

Table 7
Semi-quantitative XRD analysis of clinker phases

	Reference	R–R$_{(X < 45\ \mu m)}$	R–R$_{(45 < X < 90\ \mu m)}$	R–R$_{(X > 90\ \mu m)}$	R–B$_{(X < 45\ \mu m)}$	R–B$_{(45 < X < 90\ \mu m)}$	R–B$_{(90\ \mu m)}$	R–M$_{(X < 45\ \mu m)}$	R–M$_{(45 < X < 90\ \mu m)}$	R–M$_{(X > 90\ \mu m)}$
Phases at 1270 °C										
C_3S	++	++	++	+	++	++	+	+++	++	+
βC_2S	+	+	++	+++	++	++	+++	++	+++	+++
C_3A	++	++	+	+	++	++	++	++	++	++
C_4AF	++	++	++	++	++	++	++	++	++	+++
$CaO_{(Free)}$	+	+	+	+++	++	++	+++	+	+	+++
$C_{12}A_7$	0	0	0	+	+	+	+	0	0	+
γC_2S	–	–	–	0	–	0	0	–	–	0
Phases at 1350 °C										
C_3S	+++	+++	+++	++	+++	+++	++	+++	+++	+
βC_2S	0	+	++	++	+	+	+++	+	+	+++
C_3A	++	+	+	+	+	++	++	+	++	++
C_4AF	++	++	++	++	++	++	++	++	++	++
$CaO_{(Free)}$	+	+	+	+	+	+	++	+	+	++
Phases at 1400 °C										
C_3S	+++	+++	+++	++	+++	+++	++	+++	+++	+++
βC_2S	0	0	0	+	0	0	++	0	0	+
C_3A	+	+	+	+	+	+	+	+	++	+
C_4AF	++	++	++	++	+	+	++	++	++	++
$CaO_{(Free)}$	0	0	0	++	0	+	++	0	+	++
Phases at 1450 °C										
C_3S	+++	+++	+++	++	+++	+++	++	+++	+++	+++
βC_2S	0	0	0	+	0	0	++	0	0	+
C_3A	+	+	+	+	+	+	+	++	++	++
C_4AF	++	++	++	++	+	+	++	++	++	++
$CaO_{(Free)}$	0	0	0	+	0	0	++	0	0	++
Phases at 1500 °C										
C_3S	+++	+++	+++	+++	+++	+++	++	+++	+++	+++
βC_2S	0	0	0	0	0	0	+	0	0	0
C_3A	+	+	+	+	+	+	+	++	++	++
C_4AF	++	++	++	++	+	+	++	++	++	++
$CaO_{(Free)}$	0	0	0	+	0	0	++	0	0	+

Symbol criteria +++ (abundant), ++ (moderate), + (little) and 0 (traces).

containing ceramic waste than in the conventional product (Fig. 3A). According to the XRD results (see Table 7), reactivity was good in these raw mixes, especially considering that the reference clinker used for comparison was prepared from a mix with an optimum particle size for all components [17].

The morphological analysis provided further evidence of the lower reactivity of clinkers containing a particle size of over 90 μm. Phase distribution was highly uneven as can be seen in the micrographs in Fig. 5, where large belite clusters (indicative of non-reactivity) may be easily seen in the matrix formed.

3.2. Raw mix burnability

Raw mix burnability is related to the rate at which CaO combines during the thermal process. Burnability is evaluated in terms of chemical, physical and mineralogical parameters. Table 8 gives the free lime values obtained for the clinker prepared.

A comparison of the findings shows that burnability was good in the clinker made from raw mixes containing waste material with a particle size lower than 90 μm and comparable to the values found for reference specimen, when R–M ceramic waste was used, free lime content of the waste-based material was measured less than that of the conventional one. When the particle size was over 90 μm, burnability was rather poor, although as pointed out earlier, this fraction was particularly coarse. At clinkerization temperatures below 1400 °C, the free lime content in the R–B type clinker was higher than in all the others, confirming the lower reactivity observed in the tests discussed earlier.

Eq. (4) proposed by Miller [17], based on chemical parameters and particle size, was used to evaluate the burnability in this study:

$$CaO_{1400\ ^\circ C} = 0.31(LSF - 100) + 2.18(Ms - 1.8) + 0.33K + 0.73Q + 0.34Aq, \quad (4)$$

where LSF is the lime saturation factor, Ms is the silica modulus, K is the percentage of limestone with a particle size > 125 μm, Q is the percentage of sand > 45 μm; Aq is the percentage of clay material > 63 μm.

The value of the coefficient for Aq can be found by substituting the free lime values obtained at 1400 °C, the parameters used to prepare the raw mixes (LSF = 98% and Ms = 2.30) and the Aq content corresponding to the percentage of ceramic waste in the raw mixes (see Table 5) in Eq. (1); parameters Q and K can be disregarded because all the quartz (Q) and the limestone (K) crystals were smaller than 45 and 125 μm, respectively. The value of the coefficient is indicative of the contribution of the ceramic waste to the final free lime content in these clinkers. The values found for the Aq coefficients for each clinker are given in Table 9.

The results listed in Table 9 show that the raw mixes containing ceramic waste with a particle size lower than 90 μm had better burnability values than Miller's empirical mixes. In Miller's equation, the coefficient for the clay material fraction with a particle size lower than 63 μm is 0.34 (see Eq. (1)). This coefficient was found to be from 65% to 88% lower in the raw mixes containing ceramic waste with a particle size below 90 μm. This means that only a minor amount of the final free lime in the clinker can be attributed to the waste particles.

The coefficient was larger than Miller's in mixes with waste particles larger than 90 μm, although attention is again drawn to the fact that over 90% of the particles in this fraction were larger than 500 μm.

3.3. Minor components

Table 10 shows the results of the chemical analysis of clinkers obtained at 1450 °C. The oxide content of the principal constituents was similar in all clinkers, regardless of whether the raw mix contained ceramic waste. Differences were observed, however, in the percentage of certain elements and heavy metals present. Specifically, the clinker obtained from raw mixes with ceramic waste contained more ZnO, ZrO_2 and B_2O_3. These elements are found in tile glazes, which would explain the higher content in clinker made from such raw mixes. Table 10 also shows that the amount of ZnO and ZrO_2 in the clinker depends on the particle size and type of waste used. The ZnO content increased by more than 350% and the ZrO_2 content by from 100 to 250% as waste particle size increased from the finest ($X < 45$ μm) to the coarsest ($X > 90$ μm) fraction. For both oxides, but

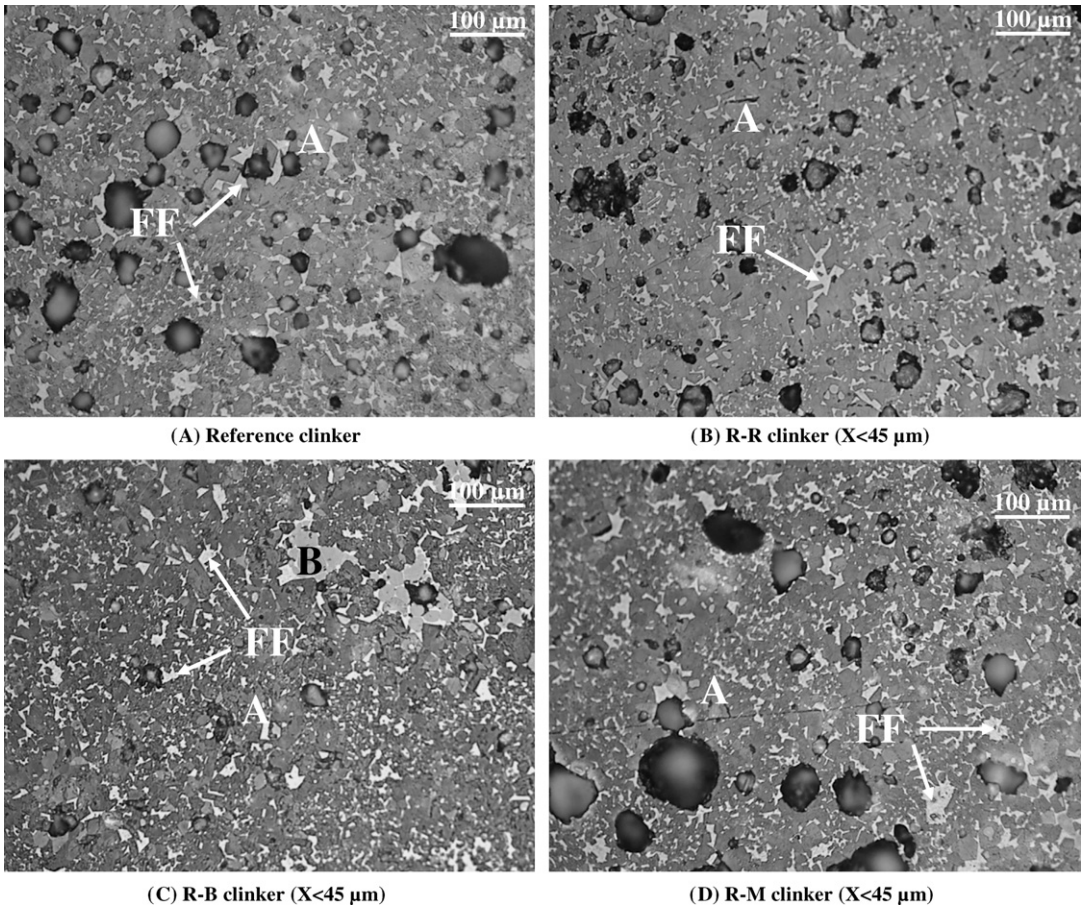

Fig. 3. Micrographs of clinker obtained at 1450 °C. Particle size of ceramic waste in raw mix: $X < 45$ μm (B = Belite; A = Alite; FF = Interstitial phase).

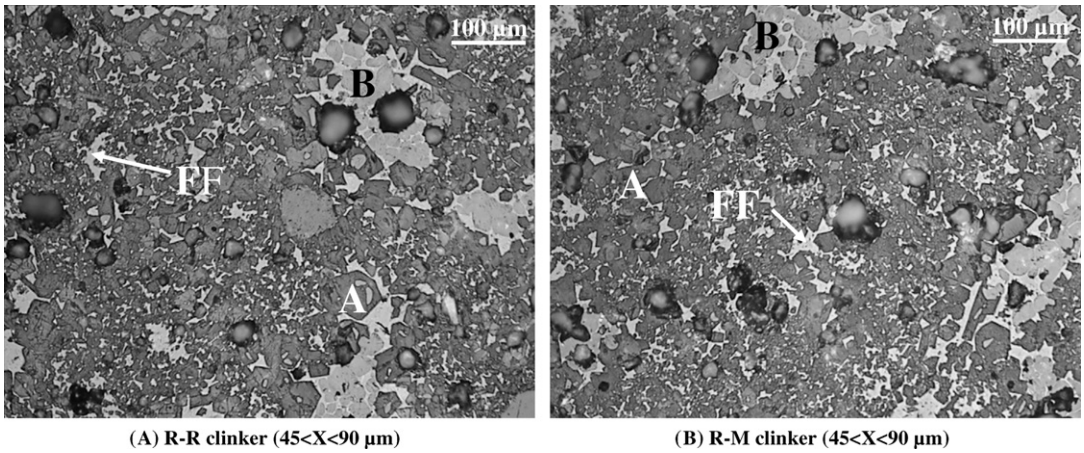

Fig. 4. Micrographs of clinker obtained at 1450 °C. Particle size of ceramic waste in raw mix: $45 < X < 90$ μm (B = Belite; A = Alite; FF = Interstitial phase).

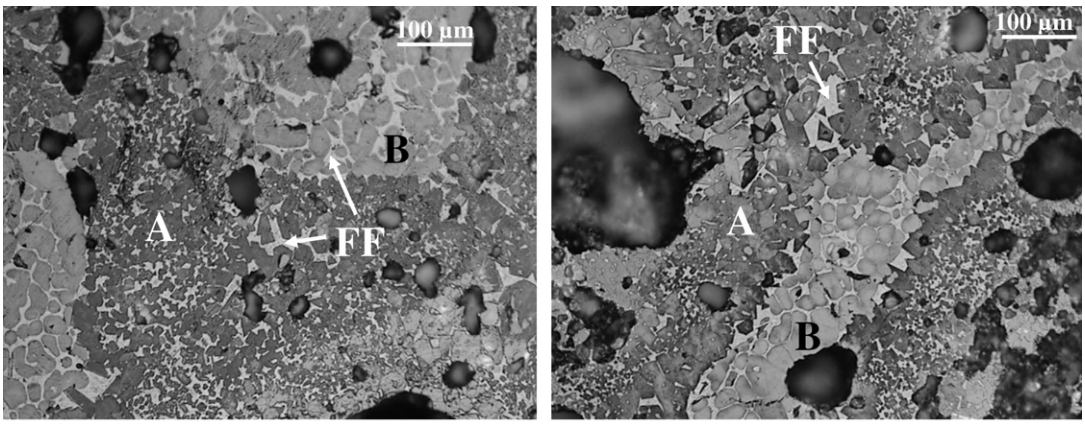

(A) R-R clinker (X>90 μm) (B) R-B clinker (X>90 μm)

Fig. 5. Micrographs of clinker obtained at 1450 °C. Particle size of ceramic waste in raw mix: $X > 90$ μm (B = Belite; A = Alite; FF = Interstitial phase).

Table 8
Clinker free lime content

Clinker	1270 °C	1350 °C	1400 °C	1450 °C	1500 °C
R–R ($X < 45$ μm)	4.36%	2.47%	1.46%	1.03%	0.55%
R–R ($45 < X < 90$ μm)	4.98%	2.95%	1.75%	0.57%	0.41%
R–R ($X > 90$ μm)	14.95%	9.55%	7.25%	6.03%	4.06%
R–B ($X < 45$ μm)	6.37%	2.37%	1.47%	1.01%	0.41%
R–B ($45 < X < 90$ μm)	8.48%	2.59%	2.19%	0.91%	0.48%
R–B ($X > 90$ μm)	23.14%	12.05%	8.66%	6.00%	7.15%
R–M ($X < 45$ μm)	4.71%	1.92%	0.85%	0.59%	0.34%
R–M ($45 < X < 90$ μm)	4.85%	2.98%	1.13%	0.89%	0.34%
R–M ($X > 90$ μm)	22.42%	9.33%	8.97%	6.7%	3.94%
Reference	4.05%	2.03%	1.59%	0.45%	0.42%

Table 9
Clinker Aq coefficients

Sample	Coefficient
R–R ($X > 45$ μm)	0.0863
R–R ($45 < X < 90$ μm)	0.1115
R–R ($X > 90$ μm)	0.5911
R–B ($X > 45$ μm)	0.0694
R–B ($45 < X < 90$ μm)	0.1195
R–B ($X > 90$ μm)	0.5691
R–M ($X > 45$ μm)	0.0289
R–M ($45 < X < 90$ μm)	0.0617
R–M ($X > 90$ μm)	0.7944

especially in the case of ZrO_2, the difference between the finest and the intermediate particle size ($45 < X < 90$ μm) was less pronounced than the difference between the intermediate and the coarsest size. The concentration of these metals was obviously much higher in the coarsest fraction of the waste. The nature of the waste also appeared to affect the concentration of these oxides, which was higher in waste R–B.

According to the literature [18,20,21], ZnO enhances raw mix reactivity, acting as a mineralizer and fusing agent. Its presence in raw mixes affects not only silicate, but also aluminate phase formation. The high concentration of this oxide in clinker obtained from ceramic waste might explain both the higher reactivity and the more abundant liquid phase observed in such mixes. ZrO_2, in turn, is known to have no substantial effect on the reactive

Table 10
Chemical composition of clinker obtained at 1450 °C (% by weight)

(wt.%)	Ref.	R–R($X < 45$ μm)	R–R($45 < X < 90$ μm)	R–R($X > 90$ μm)	R–B($X < 45$ μm)	R–B($45 < X < 90$ μm)	R–B($X > 90$ μm)	R–M($X < 45$ μm)	R–M($45 < X < 90$ μm)	R–M($X > 90$ μm)
SiO_2	20.9	20.8	21.1	20.6	21.1	21.4	21.4	21.0	21.4	21.0
Al_2O_3	5.6	5.6	5.5	5.5	5.8	5.7	5.8	5.7	5.5	5.6
Fe_2O_3	3.56	3.57	3.56	3.55	3.59	3.57	3.35	3.45	3.34	3.30
CaO	67.0	67.6	67.0	67.1	67.9	67.6	67.4	67.0	66.9	67.0
MgO	2.06	1.48	1.41	1.41	0.85	0.85	0.88	1.56	1.51	1.44
Na_2O	0.12	0.14	0.22	0.22	0.11	0.12	0.17	0.17	0.18	0.20
K_2O	0.28	0.22	0.54	0.55	0.21	0.18	0.50	0.36	0.43	0.62
TiO_2	0.21	0.20	0.21	0.21	0.21	0.21	0.21	0.18	0.18	0.18
MnO	0.04	0.01	0.01	0.01	0.01	0.01	0.01	0.01	0.01	0.01
P_2O_5	0.11	0.12	0.12	0.14	0.15	0.14	0.14	0.15	0.13	0.13
ZnO	<0.0020	0.0130	0.0240	0.0620	0.0195	0.0320	0.0990	0.0170	0.0270	0.0750
ZrO_2	<0.0020	0.0365	0.0400	0.0770	0.0210	0.0280	0.0690	0.0160	0.0198	0.0520
SO_3	0.079	0.035	0.022	0.033	0.023	0.017	0.018	0.033	0.017	0.029
PbO	<0.0020	<0.0020	<0.0020	<0.0020	<0.0020	<0.0020	<0.0020	<0.0020	<0.0020	<0.0020
BaO	0.0120	0.0170	0.0180	0.0100	<0.0020	0.0050	0.0115	0.0030	0.0080	0.0120
B_2O_3	0.0080	0.0255	0.0270	0.0260	0.0250	0.0250	0.0260	0.0220	0.0225	0.0220
Cr_2O_3	0.0015	<0.0020	<0.0020	<0.0020	<0.0020	<0.0020	<0.0020	<0.0020	<0.0020	<0.0020
V_2O_5	0.0075	0.0055	0.0065	0.0050	0.0050	0.0040	0.0050	0.0050	0.0060	0.0060
Co_3O_4	<0.0020	<0.0020	<0.0020	<0.0020	<0.0020	<0.0020	<0.0020	<0.0020	<0.0020	<0.0020
NiO	<0.0020	<0.0020	<0.0020	<0.0020	<0.0020	<0.0020	<0.0020	<0.0020	<0.0020	<0.0020
CuO	<0.0020	<0.0020	<0.0020	<0.0020	<0.0020	<0.0020	<0.0020	<0.0020	<0.0020	<0.0020
As_2O_3	<0.0020	<0.0020	<0.0020	<0.0020	<0.0020	<0.0020	<0.0020	<0.0020	<0.0020	<0.0020
Sb_2O_3	<0.0020	<0.0020	<0.0020	<0.0020	<0.0020	<0.0020	<0.0020	<0.0020	<0.0020	<0.0020
CdO	<0.0020	<0.0020	<0.0020	<0.0020	<0.0020	<0.0020	<0.0020	<0.0020	<0.0020	<0.0020

processes involved in clinker formation, although it may impact the size and shape of alite and belite crystals due to the alterations induced in the physical properties of the liquid phase [22]. According to Kakali et al. [23], the presence of this oxide in clinker may retard the initial hydration reactions and lengthen setting times. This issue is being addressed in ongoing studies.

The results for B_2O_3 (see Table 10) indicate that its content in all the clinkers was practically constant, on the order of 0.025% and therefore independent of the fraction of waste used. Nonetheless, the concentration of this oxide was around 200% higher in the alternative than in the reference clinker. Although B_2O_3 is known to be able to inhibit C_3S formation and favour belite phase stabilization that effect was not observed in the present study, where the alite content in all the experimental clinkers was comparable to the content in the reference.

The much lower chromium content in the clinker made from raw mixes containing ceramic waste was due to the absence in these mixes of sand, the component which, as Table 4 shows, had the highest chromium content. Such a low Cr content in clinker made from ceramic waste is a very promising finding in view of the present demands to reduce Cr (VI) in cement or eliminate it altogether for its deleterious effects. The results for the other minority elements analyzed indicate that this content was not affected by the composition of the cement raw mix.

4. Conclusions

The results obtained in the present study confirm the technical viability of utilizing certain types of ceramic waste as raw materials in the mixes used to manufacture Portland cement clinker. The following major conclusions may also be drawn from the study:

(a) Raw mixes containing ceramic waste with a particle size smaller than 90 μm exhibited good reactivity. The formation temperature of the liquid phase was lower and phase content higher than in the reference mix. When ceramic waste with a particle size below 45 μm was used, the solid state reactions also took place at a slightly fast rate. The mineral composition and phase distribution in the clinker obtained were comparable to the properties of clinker manufactured with conventional raw materials.

(b) The new raw mixes exhibited higher burnability than the traditional mix when the particle size of the ceramic waste was lower than 90 μm.

(c) ZnO, ZrO_2 and B_2O_3 concentration was high in the waste-containing clinker due to the presence of these oxides in tile glazing. The effect of these compounds on the hydration of the respective cements must be ascertained. At the same time, the chromium content in these clinkers was observed to be low, because raw mixes containing waste require no sand, which has relatively high chromium content.

(d) The raw mixes containing red ceramic wall tile waste (higher Fe_2O_3 content and larger amorphous phase), i.e. R–R and R–M, were found to be more reactive. The good performance of the R–M waste, indiscriminate mix of red and white ceramic wall tile, is a promising indication that the separation of different types of waste would not be necessary in order to obtain a technically acceptable material.

Acknowledgements

This study was funded by the Spanish Ministry of Education and Science (MEC) under grants for Projects CTM2004-06619-CO2-01 and 02/TECHNO.

I. García Díaz and M. Palacios benefited from pre-Ph.D. grants awarded by the MEC and the Region of Madrid (CAM), respectively, and S. Martínez-Ramírez from a "Ramón y Cajal" contract funded by the MEC and the ERDF.

References

[1] Van Oss HG, Padovani AC. Cement manufacture and the environment. Part II: Environmental challenges and opportunities. J Ind Ecol 2003;7(1):93–126.
[2] Rougemont F. Sustainable development in the cement industry: The South African record. In: Proceedings of the 11th ICCC, Durban; 2003. p. 9–18.
[3] Puertas F, Blanco-Varela MT. Empleo de combustibles alternativos en la fabricación de cemento. Efecto en las características y propiedades de los clínkeres y cementos. Mater Construcc 2004;54(274):51–64.
[4] Trezza MA, Scian AN. Waste fuels: their effect on Portland cement clinker. Cem Concr Res 2005;35(3):438–44.
[5] Monshi A, Kasiri Asgarani M. Producing Portland cement from iron and steel slags and limestone. Cem Concr Res 1999;29(9):1373–7.
[6] Goñi S, Guerrero A, Macias MaA, Peña R, Fernádez Escalante E. Empleo de materiales secundarios como materia prima de nuevos tipos de cementos. Mater Construcc 2001; 263–264:71–83.
[7] Navia R, Rivela B, Lorber KE, Méndez R. Recycling contaminated soil as alternative raw material in cement facilities: Life cycle assessment. Resour Conserv Recycling 2006;48(4):339–56.
[8] Pay-Haung Shih, Juu-En Chang, Li-Choung Chiang. Replacement of raw mix in cement production by municipal solid waste incineration ash. Cem Concr Res 2003;33(11):1831–6.
[9] Singh M, Upadhayay SN, Prasad PM. Preparation of special cements from red mud. Waste Manage 1996;16(18):665–70.
[10] Puertas F, Blanco-Varela MT, Palomo A, Vázquez T. Reactivity and burnability of raw mixes made with crystallized blast furnace slag. Part I and Part II. Zement Kalk Gips 1988;8:398–402 (12):628–31.
[11] Mehta PK. Pozzolanic and cementitious by-products. In: Proceedings of the third international conference on fly ash, silica fume, slag and natural pozzolans in concrete, Trondheim; 1989. p. 114–1, 1–43.
[12] Schwarz N, Cam H, Neithalath N. Influence of a fine glass powder on the durability characteristics of concrete and its comparison to fly ash. Cem Concr Comp 2008;30(6):486–96.
[13] Cordeiro GC, Toledo Filho RD, Tavares LM, Fairbairn EMR. Pozzolanic activity and filler effect of sugar cane bagasse ash in Portland cement and lime mortars. Cem Concr Comp 2008;30(5):410–8.
[14] Puertas F, Barba A, Gazulla MF, Gómez MP, Palacios M, Martínez-Ramírez S. Ceramics wastes as raw material in Portland cement clinker fabrication: characterization and alkaline activation. Mater Construcc 2006;56(281): 73–84.
[15] Sánchez-Roja MI, Frías M, Rivera J, Marín FP. Wastes products from prefabricated ceramic materials as pozzolanic addition. In: Proceedings of the 11th ICCC, Durban; 2003. p. 935–43.
[16] Ay N, Ünal M. The use of waste ceramic tile in cement production. Cem Concr Res 2000;30(3):497–9.
[17] Miller FM. La microscopie dans l'evaluatio de la facilité de cuisson et la clinkrisatio. Cimetns Betons Platres Chaux 1981; 731(4):212–18.
[18] Kakali G, Parissakis G. Investigation of the effect of Zn oxide on the formation of Portland cement clinker. Cem Concr Res 1995;25(1):79–85.
[19] Timashev VV. Cinétique de la clinkérisation. Structure et composition du clinker et ses phases. In: Proceedings of the VII International congress on the chemistry of cement, Paris; 1980. p. I:3/1–3/19.
[20] Kolovos K, Tsivilis S, Kakali G. The effect of foreign ions on the reactivity of the $CaO-SiO_2-Al_2O_3-Fe_2O_3$ system. Part II: Cations. Cem Concr Res 2002;32(3):463–9.
[21] Bolio-Arceo H, Glasser FP. Zinc oxide in cement clinkering: Part I. Systems $CaO–ZnO–Al_2O_3$ and $CaO–ZnO–Fe_2O_3$. Adv Cem Res 1998;10(1):25–32.
[22] Kakali G, Kasselouri V, Parissakis G. Investigation of the effect of Mo, Nb, W and Zr oxides on the formation of Portland cement clinker. Cem Concr Res 1990;20(1):131–8.
[23] Kakali G, Kasselouri V, Parissakis G. Hydration and strength development of cements produced from raw mixes containing MoO_3, Nb_2O_5, WO_3 and ZrO_2. Cem Concr Res 1989;19(6):968–72.